Sensitivity of alpha-particle–driven Alfvén eigenmodes to q-profile variation in ITER scenarios

P. Rodrigues[1], A. C. A. Figueiredo[1], L. Fazendeiro[1], J. Ferreira[1], R. Coelho[1], F. Nabais[1], D. Borba[1], N. F. Loureiro[1,2], A. R. Polevoi[3], S. D. Pinches[3], and S. E. Sharapov[4]

[1]Instituto de Plasmas e Fusão Nuclear, Instituto Superior Técnico, Universidade de Lisboa, 1049-001 Lisboa, Portugal.
[2]Plasma Science and Fusion Center, Massachusetts Institute of Technology, Cambridge, MA 02139, USA.
[3]ITER Organization, Route de Vinon-sur-Verdon, 13067 St Paul-lez-Durance Cedex, France.
[4]CCFE, Culham Science Centre, Abingdon OX14 3DB, United Kingdom.

E-mail: `par@ipfn.ist.utl.pt`

Abstract. An hybrid ideal-MHD/drift-kinetic approach to assess the stability of alpha-particle–driven Alfvén eigenmodes in burning plasmas is used to show that certain foreseen ITER scenarios, namely the $I_{\mathrm{p}} = 15$ MA baseline scenario with very low and broad core magnetic shear, are sensitive to small changes in the background magnetic equilibrium. Slight perturbations (of the order of 1%) in the total plasma current are seen to cause large variations in the growth rate, toroidal mode number, and radial location of the most unstable eigenmodes found. The observed sensitivity is shown to proceed from the very low magnetic shear values attained throughout the plasma core.

1. Introduction

Plasma heating during the burning regime in tokamak reactors will rely upon the energy of fusion-born alpha-particles that must be kept confined in order to keep the plasma hot and prevent wall damage [1]. However, such suprathermal particles can drive Alfvén Eigenmodes (AEs) unstable and be thus transported away from the plasma core, which would hamper the burning process [2, 3]. In order to predict the level of alpha-particle redistribution and loss that is expected for a given fusion scenario, the most unstable AEs need to be identified first so that their stability properties can be employed in further analysis.

Understanding the complex interplay between energetic suprathermal particles and AEs is a key step in the fusion research effort [2–4], particularly in preparation for future burning-plasma experiments. Recent research concerning ITER [5–8] has been focusing on the 15 MA baseline scenario, with on-axis safety factor close to unity and low magnetic shear throughout the plasma core [9]. In this work, an hybrid ideal-MHD/drift-kinetic plasma model is used to find how the stability properties of AEs change in response to small variations of the background magnetic equilibrium. Of particular interest are the net growth rate, wave number, and frequency of the most unstable AEs. These properties are shown to be significantly affected by small changes of the safety-factor profile, which are achieved through slight variations of the total plasma current.

2. Particle-wave interaction model

Routine stability assessments in burning plasmas can be accomplished with an hybrid MHD–drift-kinetic model of particle-wave interaction [7]. Here, ideal-MHD theory is used to describe thermal species (DT fuel ions, electrons, He ash and other impurities), whose energy distribution functions are assumed to be local Maxwellians. The radial dependence of their temperature and particle-number density is an input to the model. A similar input must also be provided for the density of the suprathermal, diluted, fusion-born alpha-particle population, which is assumed to be isotropic in pitch angle. Its energy distribution function is assumed to be described by the model [10]

$$f_{\mathrm{sd}}(E) = \frac{C_{\mathrm{N}}}{E^{3/2} + E_{\mathrm{c}}^{3/2}} \, \mathrm{erfc}\big[(E - E_0)/\Delta_{\mathrm{E}}\big], \tag{1}$$

where C_{N} is a normalization constant while E_{c}, Δ_{E}, and E_0 are radius-independent parameters, and erfc is the complementary error function.

The response of the non-Maxwellian alpha-particle population to an ideal-MHD perturbation of the thermal plasma is found solving the linearized drift-kinetic equation [11], valid in the limit

$$\omega/\Omega_\alpha \sim \big(k_\perp \rho_\alpha\big)^2 \ll 1, \tag{2}$$

with ω and $k_\perp$ the AE frequency and perpendicular wave number, whereas Ω_α and ρ_α are the alpha-particle gyro-frequency and gyro-radius. This response gives rise to a small complex correction $\delta\omega$ to the frequency ω of marginally stable AEs and the alpha-particle contribution to their growth rate is then $\gamma_\alpha = \mathrm{Im}(\delta\omega)$. A similar procedure for each thermal species j produces the corresponding Landau-damping contribution γ_j to the wave-particle energy exchange. Disregarding effects not contained in the ideal-MHD framework (e.g., Alfvén-continuum damping, radiative damping), which
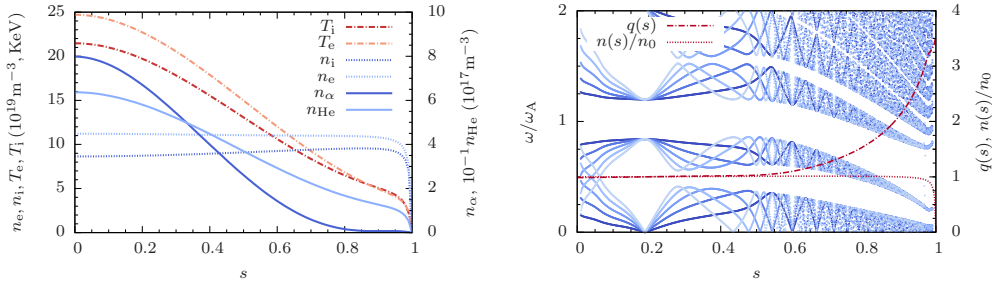
Figure 1. Radial distribution of the plasma-species densities and temperatures (left), ideal Alfvén continua for toroidal mode numbers $n = 10, \ldots, 50$ (from dark to light hues), safety factor, and normalized mass density (right).

cannot be modeled by the perturbative approach just described, the overall AE growth rate is thus $\gamma_\alpha + \sum_j \gamma_j$.

The workflow to assess the stability of a given plasma configuration is as follows [7]: a magnetic equilibrium is first computed with `HELENA` [12], using pressure and current-density profiles obtained from transport modelling, and then all possible AEs are found by intensively scanning over a frequency and wave-number range with the ideal-MHD code `MISHKA` [13], while the energy transfer between them and all plasma species is evaluated with the drift-kinetic code `CASTOR-K` [14, 15]. The computational efficiency of the `MISHKA`/`CASTOR-K` pair is the key to handle the very large number of AEs involved in such systematic stability assessments.

3. The reference case

The radial distribution of each species' particle-density and temperature for the ITER $I_{\mathrm{p}} = 15$ MA baseline scenario [9] were found with the transport code `ASTRA` [16] and are displayed in figure 1, where $s^2 = \psi/\psi_{\mathrm{b}}$, ψ is the poloidal flux, and ψ_{b} is its value at the boundary. Other relevant parameters are the on-axis magnetic field $B_0 = 5.3$ T, the minor radius $a = 2$ m, and the magnetic-axis location at $R_0 = 6.4$ m (not to be confused with the tokamak's geometric axis $R_{\mathrm{vac}} = 6.2$ m). The DT fuel mix ratio is $n_{\mathrm{D}}/n_{\mathrm{T}} = 1$ and their combined density is $n_{\mathrm{i}} = n_{\mathrm{D}} + n_{\mathrm{T}}$. Peaked temperature profiles contrast with DT-ion and electron density distributions, which are flat almost up to the plasma edge. In turn, fusion alpha-particles are mostly concentrated in the core, with an almost constant gradient $\mathrm{d}n_\alpha/\mathrm{d}s$ for $0.3 \lesssim s \lesssim 0.5$.

Flat mass-density distributions up to the plasma edge, like the one plotted in figure 1, contribute to the closing of the frequency gaps in the Alfvén continuum arising from the coupling between distinct poloidal harmonics. Consequently, AEs with frequencies in such gaps can hardly extend towards the plasma boundary without interacting with the Alfvén continuum and thus undergo significant damping. This property acts as a filter regarding the type of AEs that can be found for the particular plasma state being considered. Actually, the safety-factor profile also depicted in figure 1 (right panel) is almost flat in the core region ($s \lesssim 0.5$), yielding well separated gaps for toroidal mode numbers $n \gtrsim 10$. Highly localized low-shear toroidicity-induced AEs (LSTAEs), with only two dominant poloidal harmonics, are therefore expected to arise in the core. Conversely, on the outer half of the plasma the magnetic shear is higher, radial gap separation is smaller, and AEs become broader, encompassing
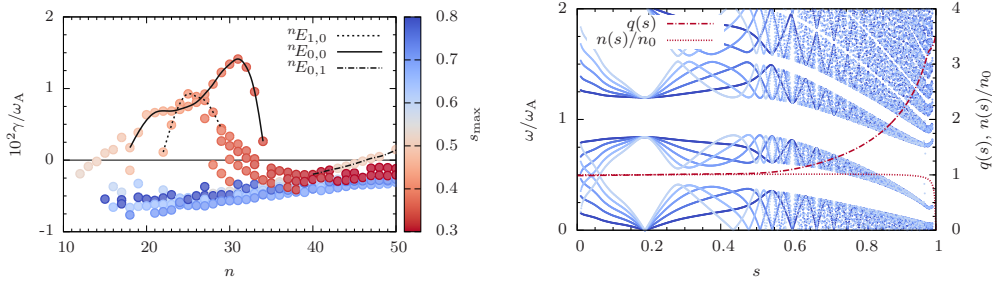
Figure 2. Distribution of the normalized growth rate γ/ω_A by n for I_{ref}, with each TAE colored by the radial location of its maximum amplitude, and three TAE families identified by dotted, solid, and dash-dotted lines (left). Example eigenfunctions of the AE families ${}^nE_{0,1}$, ${}^nE_{1,0}$, and ${}^nE_{0,0}$ (right), with baselines at their normalized frequencies (filled curves) and their corresponding ideal Alfvén continua (solid, dotted, and dash-dotted lines).

a large number of poloidal harmonics and extending to the edge. In so doing, they interact with the Alfvén continuum and are thus excluded from further analysis, which will be dominated by $n \gtrsim 10$ highly localized LSTAEs.

The $(\omega, \mathbf{k})$-space scan carried out by `MISHKA` finds the radial structure of all AEs with toroidal number n in the range $1 \leqslant n \leqslant 50$ and poloidal harmonics $n - 1 \leqslant m \leqslant n + 15$. The upper limit for n is set by the drift-kinetic ordering in (2) as

$$k_\perp \rho_\alpha \lesssim 1, \quad \text{whence} \quad n \lesssim (s/q)/(\rho_\alpha/a) \approx 50, \tag{3}$$

with $\rho_\alpha/a \approx 10^{-2}$ the normalized alpha-particle gyro-radius, $k_\perp \sim (nq)/(as)$, $q \approx 1$, and $s \approx 0.5$. For each n, the frequency range $0 \leqslant \omega/\omega_A \leqslant 1$ [where $\omega_A = V_A/R_0$, with V_A the on-axis Alfvén velocity] is sampled in small steps of size 2×10^{-5}. Next, `CASTOR-K` evaluates the energy exchange between every AE found and each of the plasma species considered, yielding the corresponding growth (or damping) rate. The parameters of the energy distribution-function model in (1) for the fusion-born alpha particles were taken at a radial location ($s \approx 0.4$) near the maximum gradient of their density profile, yielding the values $E_c = 730$ KeV, $\Delta_E = 50$ KeV, and $E_0 = 3.5$ MeV.

The stability assessment is summarized in figure 2 (left panel) for the reference scenario where the plasma current I_p takes the reference value $I_{ref} = 15$ MA and the on-axis safety factor is $q_{ref} = 0.987$. This is essentially a subset of previous results [7], here restricted to toroidicity-induced AEs (TAEs) to make the presentation of results clearer (whence the upper limit $\omega/\omega_A \leqslant 1$ set on the AEs' frequency). The most unstable TAEs found have $20 \lesssim n \lesssim 30$ and lie in the core ($0.3 \lesssim s_{max} \lesssim 0.5$, with s_{max} the location of their maximum amplitude), where dn_α/ds is highest and the magnetic shear is lowest. Conversely, AEs located in the outer half of the plasma ($0.5 \lesssim s_{max} \lesssim 0.8$) are mostly stable due to smaller values of the alpha-particle density n_α and its gradient dn_α/ds.

Three lines are plotted in figure 2 (left) connecting TAEs belonging to three families that will play a key role in the ensuing discussion. These families are denoted as ${}^nE_{l,p}$, meaning that their members are LSTAEs with even (E) parity and l zeros, with p being the difference between the first dominant poloidal harmonic and the toroidal number n. A member of each family has its radial structure depicted in the right panel of figure 2, where they can be identified by their respective Alfvén continua.
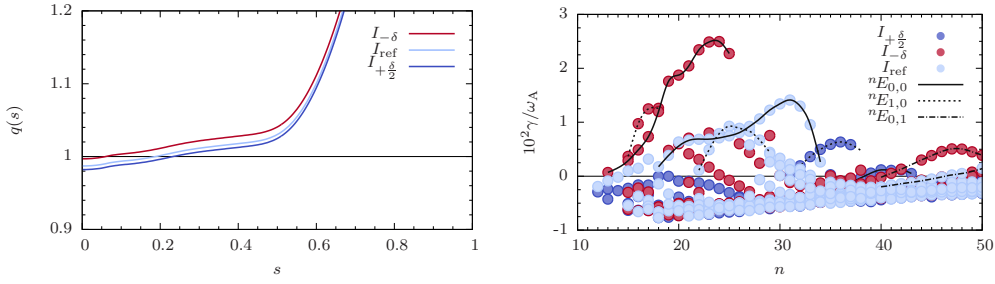
Figure 3. Left: Safety-factor profiles for the reference plasma current and two slightly different I_p values. Right: Distribution of the normalized growth rate γ/ω_A by n for the three plasma-current values, with indication of the three TAE families.

4. Small changes in magnetic equilibria

The reference value $I_\mathrm{ref} = 15$ MA considered in the stability analysis that led to figure 2 is only nominal. In practice, ITER operation under this baseline scenario will exhibit values of the plasma current which are close, but of course not rigorously equal to, the reference I_ref. To explore the dependence of the AE stability on this uncertainty, two different magnetic equilibria are next considered, in addition to the reference one discussed in the previous Section. These equilibria are obtained by changing I_p from I_ref by the small amounts $-\delta$ and $\delta/2$, with $\delta = 0.16$ MA, whilst keeping the same equilibrium profiles $p'(\psi)$ and $f(\psi)f'(\psi)$. The resulting safety-factor profiles are plotted in figure 3 (left), along with the reference one for comparison. As expected, the on-axis safety factor value q_0 changes only slightly by circa 1% and 0.5% respectively, thus following the magnitude of the I_p variation away from I_ref. Moreover, the safety-factor derivative in the plasma core is kept almost unchanged in the two cases, with $q_0' \approx 0.07$.

The consequences concerning the stability properties are displayed in figure 3 (right), where the small variations ($\sim 1\%$) in I_p or q_0 are seen to cause large changes in the toroidal number ($\sim 20\%$) and normalized growth rate ($\sim 50\%$) of the most unstable AEs. Decreasing I_p (and thus raising q_0) pushes the most unstable AE families ($^nE_{0,0}$ and $^nE_{1,0}$) towards lower n and up to larger growth rates. A slight increase in I_p yields the opposite. In both cases, the most unstable AEs are still even LSTAEs.

This extreme sensitivity to small changes in the background magnetic equilibrium can be understood with the aid of the three conditions:

$$q = q_0 + q_0's, \tag{4}$$

$$q = 1 + \frac{1}{2n}, \tag{5}$$

and

$$k_\perp \Delta_\mathrm{orb} = \left(\frac{nq}{as}\right)\left(\frac{aq}{\varepsilon\tilde\Omega}\right) \sim 1. \tag{6}$$

The first one is a linear representation of the safety factor profile in the low-shear core and the second defines the resonant surface of each TAE in the $^nE_{l,0}$ families. In turn, the third relation is a condition for efficient drive, with $\Delta_\mathrm{orb} \sim (aq)/(\epsilon\tilde\Omega)$ the orbit width of an alpha-particle travelling at the Alfvén velocity with a very small

pitch angle, $\tilde{\Omega} = \Omega_\alpha/\omega_A$ its normalized gyro-frequency, and $\varepsilon = a/R_0$ the equilibrium inverse aspect ratio. Together, these three equations set the three variables n, q, and s (respectively, toroidal mode number, safety factor, and radial location) corresponding to the most unstable AEs in terms of the four parameters q_0, q_0', ε, and $\tilde{\Omega}$. Solving for the toroidal number, one gets the relation

$$n + \frac{1 - 2\zeta}{4n} + 1 = \zeta(1 - q_0), \tag{7}$$

which is written in terms of the dimensionless number

$$\zeta \equiv \frac{\varepsilon\tilde{\Omega}}{q_0'} = \left(\frac{q}{q_0'}\right) \Big/ \left(\frac{\Delta_{\text{orb}}}{a}\right). \tag{8}$$

Subtracting from equation 7 its evaluation with the values n_{ref} and q_{ref} corresponding to the reference case, gives

$$\left(1 + \frac{2\zeta - 1}{4n_{\text{ref}}\, n}\right)(n - n_{\text{ref}}) = -\zeta\big(q_0 - q_{\text{ref}}\big), \tag{9}$$

which relates a variation of the on-axis safety factor with a corresponding change in the toroidal number of the most unstable LSTAEs.

For the ITER scenario under consideration, parameters are $q_0' \approx 0.07$, $\varepsilon \approx 0.3$, and $\tilde{\Omega} \approx 230$, whence $\zeta \approx 10^3$. On the other hand, $n \sim n_{\text{ref}} \sim 30$ and therefore $(2\zeta - 1)/(4n_{\text{ref}}n) \sim 1/2$. Because the prefactor in the left-hand side of equation (9) is of the order of unity, it is the large value attained by ζ in the right-hand side that forces small changes of the on-axis safety factor to cause large variations $n - n_{\text{ref}}$. Also, one easily checks that increasing q_0 above q_{ref} lowers n below n_{ref} and conversely, as observed in figure 3. Moreover, the conditions in equations (4), (5), and (6) relate the radial location s of the most unstable AE with its toroidal number as

$$\varepsilon\tilde{\Omega}s = n\left(1 + \frac{1}{2n}\right)^2, \tag{10}$$

which predicts its displacement towards the core as q_0 increases and n drops according to equation (9). As this happens, the AE growth rate rises due to the larger number of alpha-particles found as it moves inwards within the small region $0.3 \lesssim s \lesssim 0.4$, where dn_α/ds is negative and almost constant (figure 1). The consequences of decreasing q_0 (or raising I_{p}) are likewise explained.

The contribution of the alpha-particle population to the AEs growth rate is [11]

$$\gamma_\alpha \propto \omega\frac{\partial f_\alpha}{\partial E} - n\frac{\partial f_\alpha}{\partial P_\phi}, \tag{11}$$

where $f_\alpha(E, P_\phi)$ is the unperturbed distribution function and

$$P_\phi = \frac{\psi_{\text{b}}}{B_0 R_0^2}s^2 + \frac{1}{\tilde{\Omega}}\frac{RB_{(\phi)}}{R_0 B}\frac{v_\parallel}{V_A} \tag{12}$$

is the normalized toroidal canonical momentum of a particle moving with velocity $v_\parallel$ parallel to a magnetic field with toroidal component $B_{(\phi)}$ and magnitude B. Because the derivative of (1) with respect to E is always negative, alpha-particle drive results from the P_ϕ gradient that relates to the radial derivative as

$$\frac{2\psi_{\text{b}}}{B_0 R_0^2}\frac{\partial f_\alpha}{\partial P_\phi} \approx \frac{1}{s}\frac{\partial f_\alpha}{\partial s} \tag{13}$$
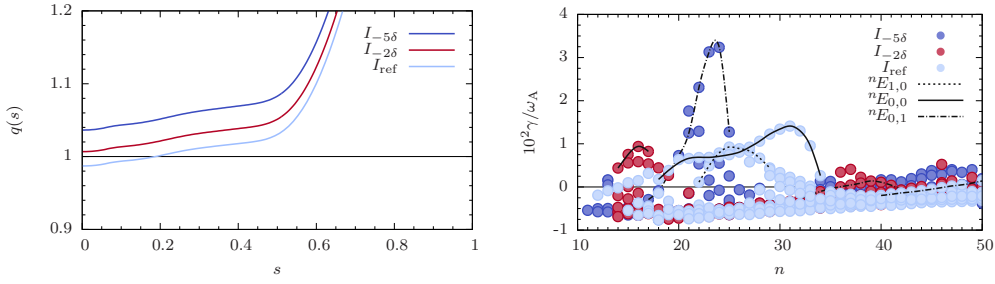
Figure 4. Safety-factor profiles for the reference plasma current and two other I_p values (left). Distribution of the normalized growth rate γ/ω_A by n for the three plasma-current values, with indication of the three TAE families.

if only lowest-order terms in $1/\tilde{\Omega}$ are kept. Replacing equations (6) and (13) in (11) and discarding the energy-gradient term, the AEs radial location cancels out and one obtains

$$\gamma_\alpha \propto -\frac{\varepsilon\tilde{\Omega}}{q^2}\frac{\partial f_\alpha}{\partial s}. \tag{14}$$

Therefore, it may be asked if pushing unstable AEs further into the core, and consequently out of the region where the gradient $\mathrm{d}n_\alpha/\mathrm{d}s$ is strongest, may reduce γ_α and thus result in their stabilization. Such inward push is achieved by slightly increasing q_0 (hence reducing I_p), which forces n in equation (9) and s in equation (10) to drop.

To address this question, two additional magnetic equilibria are considered with plasma currents $I_{-2\delta}$ and $I_{-5\delta}$ corresponding, respectively, to reductions of size 2δ and 5δ of the reference value I_ref. Their safety-factor profiles are plotted in figure 4 (left) and q_0 now increases by 2% and 5% with respect to q_ref. As a consequence, the surface $q = 1$ is removed from the plasma and solutions of the AE families ${}^nE_{l,0}$ can exist for low n only.

The new stability assessment is summarized in figure 4 (right panel). According to predictions, AE families ${}^nE_{l,0}$ are pushed to lower n and eventually vanish. For $I_{-2\delta}$ and before vanishing, AEs in the family ${}^nE_{0,0}$ have their growth rate reduced by 30% when compared to the reference case. The growth-rate reduction with respect to the case $I_{-\delta}$ is even larger. However, the AE family ${}^nE_{0,1}$ whose resonant surfaces are located at $q = 1 + \frac{3}{2n}$ is also brought to lower n and inwards from its reference radial location. For $I_{-5\delta}$ these AEs are located near the maximum gradient $\mathrm{d}n_\alpha/\mathrm{d}s$ and their normalized growth rate peaks, accordingly, at 3.2% for $n = 24$. In this way, efforts to stabilize AEs by moving them out of the strong density-gradient region are thwarted by the destabilization of AE families previously stable or weakly unstable.

5. Conclusions

In summary, an hybrid ideal-MHD/drift-kinetic model was used to show that the stability properties of ITER $I_\mathrm{p} = 15$ MA baseline scenario are significantly sensitive to small changes in the plasma current or, equivalently, in the on-axis safety factor. Such small variations were shown to cause large changes in the growth rate, toroidal number, and radial location of the most unstable AEs. This sensitivity is not an artificial feature of the ideal-MHD/drift-kinetic model employed to describe the interaction between

plasma species and AEs. On the contrary, it was shown to proceed from the large value attained by the dimensionless parameter ζ, which is caused by the combination of large alpha-particle gyro-frequency [in equation (6)] with very low magnetic shear [in equation (4)] throughout a substantial domain within the plasma core.

Low magnetic-shear profiles are expected to take place during planned ITER operation due to sawtooth activity, which periodically redistributes the toroidal current density within a large mixing region that may extend to about half of the plasma minor radius because safety-factor values at the boundary are low ($q_{\rm b} \sim 3$) [17, 18]. On the other hand, low magnetic shear was found to play an important role in the nonlinear stabilization of microturbulence by suprathermal pressure gradients [19]. As such, low magnetic shear may become advantageous in its own right, particularly in large fusion devices where sheared rotational momentum (employed to mitigate or suppress microturbulent transport [20, 21]) is difficult to achieve but suprathermal alpha particles produced in fusion reactions are plenty.

If the large sensitivity of low magnetic-shear plasma configurations found in this work is still present in nonlinear analysis, then detailed simulations (e.g., suprathermal particle transport and redistribution by nonlinear interaction with AEs) carried out in such circumstances should take this fact into account, allowing a reasonable range of inputs in order to capture eventual large changes in their results. Moreover, strong operational consequences should also be expected, as such sensitivity would imply that AE stability is, in fact, unpredictable given the extreme accuracy levels with which $I_{\rm p}$ would have to be known.

Acknowledgments

References

[1] Fasoli A, Gormenzano C, Berk H, Breizman B, Briguglio S, Darrow D, Gorelenkov N, Heidbrink W, Jaun A, Konovalov S, Nazikian R, Noterdaeme J M, Sharapov S, Shinohara K, Testa D, Tobita K, Todo Y, Vlad G and Zonca F 2007 *Nucl. Fusion* **47** S264
[2] Breizman B N and Sharapov S E 2011 *Plasma Phys. Control. Fusion* **53** 054001
[3] Gorelenkov N, Pinches S and Toi K 2014 *Nucl. Fusion* **54** 125001
[4] Sharapov S, Alper B, Berk H, Borba D, Breizman B, Challis C, Classen I, Edlund E, Eriksson J, Fasoli A, Fredrickson E, Fu G, Garcia-Munoz M, Gassner T, Ghantous K, Goloborodko V, Gorelenkov N, Gryaznevich M, Hacquin S, Heidbrink W, Hellesen C, Kiptily V, Kramer G, Lauber P, Lilley M, Lisak M, Nabais F, Nazikian R, Nyqvist R, Osakabe M, von Thun C P, Pinches S, Podesta M, Porkolab M, Shinohara K, Schoepf K, Todo Y, Toi K, Zeeland M V,

Voitsekhovich I, White R, Yavorskij V, TG I E and Contributors J E 2013 *Nucl. Fusion* **53** 104022

[5] Pinches S D, Chapman I T, Lauber P W, Oliver H J C, Sharapov S E, Shinohara K and Tani K 2015 *Phys. Plasmas* **22** 021807

[6] Lauber P 2015 *Plasma Phys. Control. Fusion* **57** 054011

[7] Rodrigues P, Figueiredo A, Ferreira J, Coelho R, Nabais F, Borba D, Loureiro N F, Oliver H and Sharapov S 2015 *Nucl. Fusion* **55** 083003

[8] Figueiredo A C A, Rodrigues P, Borba D, Coelho R, Fazendeiro L, Ferreira J, Loureiro N F, Nabais F, Pinches S D, Polevoi A and Sharapov S E 2016 Comprehensive evaluation of the linear stability of Alfvén eigenmodes driven by alpha particles in an ITER baseline scenario *Nucl. Fusion* to be submitted

[9] Polevoi A R, Medvedev S Y, Mukhovatov V S, Kukushkin A S, Murakami Y, Shimada M and Ivanov A A 2002 *J. Plasma Fusion Res. SERIES* **5** 82

[10] Pinches S, Appel L, Candy J, Sharapov S, Berk H, Borba D, Breizman B, Hender T, Hopcraft K, Huysmans G and Kerner W 1998 *Comp. Phys. Comm.* **111** 133 – 149

[11] Porcelli F, Stankiewicz R, Kerner W and Berk H L 1994 *Phys. Plasmas* **1** 470–480

[12] Huysmans G, Goedbloed J and Kerner W 1991 *Int. J. Mod. Phys.* **2** 371

[13] Mikhailovskii A B, Huysmans G T A, Kerner W O K and Sharapov S E 1997 *Plasma Phys. Rep.* **23** 844

[14] Borba D and Kerner W 1999 *J. Comput. Phys.* **153** 101 – 138

[15] Nabais F, Borba D, Coelho R, Figueiredo A, Ferreira J, Loureiro N F and Rodrigues P 2015 *Plasma Sci. Technol.* **17** 89

[16] Pereverzev G and Corrigan G 2008 *Comp. Phys. Comm.* **179** 579–585

[17] Porcelli F, Boucher D and Rosenbluth M N 1996 *Plasma Phys. Control. Fusion* **38** 2163

[18] Hender T, Wesley J, Bialek J, Bondeson A, Boozer A, Buttery R, Garofalo A, Goodman T, Granetz R, Gribov Y, Gruber O, Gryaznevich M, Giruzzi G, Günter S, Hayashi N, Helander P, Hegna C, Howell D, Humphreys D, Huysmans G, Hyatt A, Isayama A, Jardin S, Kawano Y, Kellman A, Kessel C, Koslowski H, Haye R L, Lazzaro E, Liu Y, Lukash V, Manickam J, Medvedev S, Mertens V, Mirnov S, Nakamura Y, Navratil G, Okabayashi M, Ozeki T, Paccagnella R, Pautasso G, Porcelli F, Pustovitov V, Riccardo V, Sato M, Sauter O, Schaffer M, Shimada M, Sonato P, Strait E, Sugihara M, Takechi M, Turnbull A, Westerhof E, Whyte D, Yoshino R, Zohm H, the ITPA MHD D and Group M C T 2007 *Nucl. Fusion* **47** S128

[19] Citrin J, Jenko F, Mantica P, Told D, Bourdelle C, Garcia J, Haverkort J W, Hogeweij G M D, Johnson T and Pueschel M J 2013 *Phys. Rev. Lett.* **111**(15) 155001

[20] Burrell K H 1997 *Phys. Plasmas* **4** 1499–1518

[21] Doyle E, Houlberg W, Kamada Y, Mukhovatov V, Osborne T, Polevoi A, Bateman G, Connor J, Cordey J, Fujita T, Garbet X, Hahm T, Horton L, Hubbard A, Imbeaux F, Jenko F, Kinsey J, Kishimoto Y, Li J, Luce T, Martin Y, Ossipenko M, Parail V, Peeters A, Rhodes T, Rice J, Roach C, Rozhansky V, Ryter F, Saibene G, Sartori R, Sips A, Snipes J, Sugihara M, Synakowski E, Takenaga H, Takizuka T, Thomsen K, Wade M, Wilson H, Group I T P T, Database I C, Group M T, Pedestal I and Group E T 2007 *Nucl. Fusion* **47** S18